ACS APPLIED MATERIALS & INTERFACES

Research Article

www.acsami.org

Induction of Myogenic Differentiation of Human Mesenchymal Stem Cells Cultured on Notch Agonist (Jagged-1) Modified Biodegradable Scaffold Surface

Feng Wen,[†] Hui Kian Wong,[†] Chor Yong Tay,[†,§] Haiyang Yu,[†] Huaqiong Li,[†] Ting Yu,[‡] Ajay Tijore,[†] Freddy Yin Chiang Boey,[†] Subbu S. Venkatraman,[†] and Lay Poh Tan*[,†]

[†]Division of Materials Technology, School of Materials Science and Engineering, Nanyang Technological University, 50 Nanyang Avenue, 639798 Singapore

[‡]Division of Systems and Engineering Management, School of Mechanical and Aerospace Engineering, Nanyang Technological University, 50 Nanyang Avenue, 639798 Singapore

Supporting Information

ABSTRACT: Engineered scaffold surface provides stem cells with vital cues that could determine the eventual fate of stem cells. In this work, biodegradable poly(L-lactide-*co*-ε-caprolactone) (PLCL) scaffold conjugated with Notch agonist-Jagged-1(JAG) peptide (2.1 kDa) was prepared to initiate myogenic differentiation of human mesenchymal stem cells (hMSCs). The scaffold surface was activated with oxygen plasma and acrylic acid was engrafted via UV polymerization to form a surface bearing carboxylic groups. JAG peptide was subsequently immobilized onto the carboxylated scaffold surface. Surface chemistry and topography were examined using attenuated total reflection Fourier transform infrared, X-ray photoelectron spectroscopy, and atomic force microscopy. Quantitative real time polymerase chain reaction analysis revealed activation of the Notch pathway; furthermore, several specific markers associated with myogenic but not osteogenic differentiation were shown to be up-regulated in hMSCs cultured on the engineered surface. The pro-myocardial effect of surface bound JAG peptide was further affirmed via immunodetection of the distinct myocardial marker, cardiac troponin T. Collectively, our results suggest that PLCL conjugated JAG peptide is a viable strategy to enhance the functional potential of scaffolds to be used as a bioengineered cardiac patch in myocardial infarction repair.

KEYWORDS: *biointerfaces, surface modification, functionalization of polymers, biodegradable, tissue engineering, peptides*

INTRODUCTION

Heart failure is a major health problem and the leading cause of morbidity in both industrialized nations and the developing world.[1,2] An important cause of heart failure is myocardial infarction. After myocardial infarction, the necrotic tissue is unable to be reconstituted and initiates a detrimental cascade of events, including formation of a noncontractile scar, ventricular wall thinning, and eventually heart failure. Currently, the only viable therapy for heart failure that addresses the fundamental problem of cardiomyocytes loss is cardiac transplantation;[3] however, this option is restricted by severe scarcity of available donor hearts. In addition, the side effects of life-long immunosuppression and cardiac allograft vasculopathy limit quality of life and long-term graft function.[4]

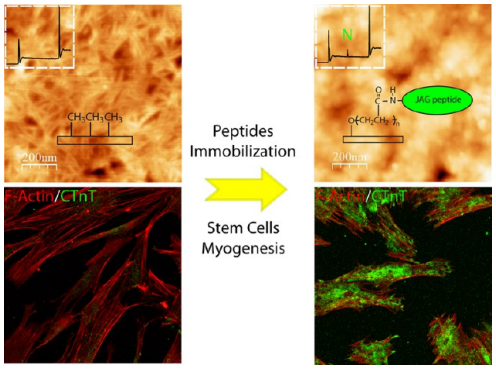

The discoveries on the regenerative potential of stem and progenitor cells have sparked interest in stem-cell therapy for treating and preventing heart failure.[5,6] Human mesenchymal stem cells (hMSCs), which can easily be isolated from an increasing number of adult tissues and are relatively privileged in terms of immune compatibility, make them attractive as a possible cell source for cardiac repair.[7,8] Studies with myocardial infarcted models have reported encouraging but limited success in recovery of infarcted myocardium function through stem cell transplantation therapy.[7,9] Direct cells injection into infarcted myocardium has been intensively investigated for myocardial regeneration. However, studies show the rates of injected cells retention and cell survival in recipient myocardium after 1 week of implantation are very low.[10,11] The possible reasons are (a) the available space in thinned ventricle wall (as a result of pathological remodelling) is limited to enable it to engraft large amount of injected cells,[12] (b) the hostile scar microenvironment is compromised due to chronic shortage of oxygen and nutrients,[13] and (c) the dense

Received: October 16, 2013
Accepted: January 10, 2014
Published: January 10, 2014

   dx.doi.org/10.1021/am4045635 | ACS Appl. Mater. Interfaces 2014, 6, 1652−1661

fibrosis in the scar tissue may act as a formidable physical barrier to inhibit cell homing and proliferation.[3] Moreover, it was reported that only a small fraction of the transplanted cells would differentiate into the myogenic lineage.[12,14] This could, in turn, reduce the clinical efficacy of this therapy for myocardial infarction treatment. Another major consideration would be the safety aspect. hMSCs lack the ability to form teratomas but may differentiate into an undesired cell type,[15] which could impair recovery of heart function as well. Therefore, some degree of myogenic differentiation of hMSCs prior to transplantation would result in a higher clinical efficacy for cardiac repair, as well as reduce the risk of undesired lineages commitment. To overcome the above limitations, scaffold-based cell delivery was proposed as an alternative strategy for myocardial infarction treatment recently, and several reports have demonstrated it could facilitate cell retention and survival by providing temporal structural support.[11,13,16,17] However, the real-time differentiation control of delivery cells is not well documented.

The Notch signaling pathway has been demonstrated to play a critical role during mammalian cardiac development.[18,19] Notch signaling is activated after the interaction of one of the four Notch receptors (Notch-1−4) with ligands of the Jagged (Jagged-1−2) or Delta-like (Delta-like-1, 3, and 4) family. Ligand−receptor interaction mediated activation directs the conversion of CSL (CBF1, Su(H) and LAG-1) proteins from repressors to transcriptional activators, and subsequent up-regulation of downstream targets (e.g., HES gene).[20,21] Experimental evidence indicated that Notch signaling can inhibit osteogenic differentiation of bone marrow mesenchymal progenitors through HES proteins, which diminished Runx2 transcriptional activity via physical interaction.[22] Conversely, activation of Notch pathway has been shown to trigger pro-myogenic events. For instance, cardiac progenitor cells differentiation can be initiated via target gene Nkx2.5 associated Notch dependent pathway,[23] which prompt cardiac marker gene expression in MSCs cocultured with cardiomyocytes.[24] Notch signaling is known to be exquisitely sensitive to dosage, developmental timing, and cellular context. The predominant effect of an exogenous Notch ligand would depend on the relative concentrations of endogenous and exogenous ligands. Thus, it would result in different dose−response relationships in different cells and tissues.[25] Notch signaling modulates transcription in several cell types, but whether it exerts an inhibitory or inductive role in the myogenic differentiation of hMSCs cultured alone remains to be elucidated.

In the field of tissue engineering and regenerative medicine, considerable effort has been devoted toward the design of new biomaterials with the aim to deliver cell regulatory signals in a spatial and temporal controlled fashion and serve as powerful component of artificial cell niche to direct cell fate.[26−31] There are several reported approaches to deliberate the activation of Notch signaling events such as coculturing with cells over-expressing JAG protein;[32] culturing in medium containing soluble JAG protein/peptide;[24,33] culturing on substrate which surface was immobilized with JAG protein.[20,23,34−36] In this report, we document the first usage of JAG peptides conjugated onto a polymeric scaffold to trigger the Notch signaling cascade. Our adopted approach of covalent immobilization of the JAG peptide offers an advantage over physical entrapment, since it enhances the stability of the peptides, and ensures that the effects are localized within the scaffold itself, rather than the surrounding tissue.[37] Moreover, another advantage of using peptide over proteins is that the former can be manufactured with conformational stability and functionalized easily due to the nonexistence of the tertiary folding and proteinase contamination. Therefore, we hypothesized that surface immobilization of Notch agonist−JAG peptide onto the biodegradable scaffolds could induce myogenic differentiation of hMSCs through activation of Notch pathway.

We engineered the surface of a biodegradable polymeric scaffold through immobilization of JAG peptide to activate the Notch signaling in hMSCs. Strikingly, we observed pro-myogenic effects of the engineered scaffold as shown by up-regulation of several myogenic differentiation key markers in hMSCs in a dose-dependent manner. We assessed the activity of Notch pathway in hMSCs through analysis of Notch and Notch pathway downstream gene expression. The induction toward myogenic differentiation of hMSCs cultured on surface of engineered scaffolds was assessed by analysis of gene expression and immunocytochemistry for several myogenic markers associated with myogenesis.

EXPERIMENTAL SECTION

Materials. All reagents were used as received except acrylic acid (AAc), which was used after vacuum distillation.[38] Poly(L-lactide-*co*-ε-caprolactone) (PLCL) was purchased from Purac Biomaterials, Lincolnshire, IL (PURASORB, 7015). 2,2-Diphenyl-1-picrylhydrazyl (DPPH), 1-Ethyl-3-[3-dimethylaminopropyl] carbodiimide hydrochloride (EDC), 2-(N-morpholino) ethanesulfonic acid (MES), and Toluidine blue O (TBO) were purchased from Sigma-Aldrich. *N*-hydroxysulfosuccinimide (sulfo-NHS) was from Research Instruments (Pierce). Recombinant form of human JAG protein was purchased from R&D system with a molecular mass 170−180 kDa by SDS-Page under reducing conditions. Synthetic JAG peptide (2.1 kDa) was purchased from StemRD. The amino acid sequence of this peptide was CDDYYYGFGCNKFCRPR, which is part of the DSL region, and highly conserved in human Jagged-1 protein.[25,33]

PLCL Scaffold Preparation. PLCL scaffolds (thickness = 110.3 ± 16.5 μm) were prepared by the solvent cast method as previous report.[39] The PLCL scaffolds were characterized with a thermogravimetric analyzer (TA Instruments) to validate the complete removal of solvent and thickness gauge (Elcometer) to measure the thickness of the cast scaffolds.

Peptide Immobilization. Peptide immobilization process was carried out as previous reports with some modifications.[38] In the first step, surface of PLCL scaffolds were activated through formation of free radicals. PLCL scaffolds were activated with radio frequency glow-discharge oxygen plasma (PX250, 100W, 13.6 MHz, March Systems). The samples were treated for 30 s at an oxygen pressure of 0.2 Torr and flow rate of 22 sccm. The plasma activated surfaces were then exposed in air for about 10 min to induce the formation of hydroperoxide groups on samples surface. In the second step, acrylic acid was polymerized on the surface under the effects of hydroperoxide and UV energy to form scaffold bearing carboxylic groups. The concentration of AAc solution used was varied from 0 to 15% (v/v). After AAc solution was bubbled by argon gas for 30 min, plasma activated samples with AAc solution were clipped between two quartz slides (Pelco International, CA) and then subjected to UV irradiation by a UV lamp (8W, Vilber Lourmat, France) with a filter of 365 nm and an intensity of 720 $\mu W/cm^2$ for 30 min. After polymerization, samples were taken out, washed extensively with deionized water, and finally dried in a vacuum desiccator (After this step, the scaffolds henceforth referred to as P-AAc). Finally, the surface immobilization of peptides were carried out using a 'two steps' EDC and sulfo-NHS chemistry as our previous report.[40] Serials concentrations of JAG peptide were used in immobilization process. JAG peptides were immobilized on scaffolds through formation peptide bonds between carboxylic groups on the surface of scaffolds and amine groups in peptides (after this step, the scaffolds henceforth referred to as P-JAG).

The amounts of free radicals on PLCL generated after plasma surface activation was quantified by a DPPH assay.[41] The concentration of surface accessible carboxylic groups on P-AAc was quantified by a TBO assay,[38] and the amount of JAG peptides on P-JAG surface was quantified by X-ray photoelectron spectroscopy (XPS) analysis.

Physiochemical Characterization of Scaffold Surface. The surface chemistry of scaffolds was examined by attenuated total reflection Fourier transform infrared (ATR-FTIR) and XPS. ATR-FTIR spectra of PLCL, P-AAc, and P-JAG were measured on a PerkinElmer Spectrum GX Fourier transform infrared spectrometer (PerkinElmer Inc., Waltham, MA, U.S.A.). XPS was performed on a Kratos Axis Ultra instrument using monochromated Al Kα radiation (1,486.71 eV), a 5 mA emission current, a 15 kV anode potential, and a charge-compensating electron flood. The base pressure was 1×10^{-9} Torr and the working pressure was 7×10^{-9} Torr. The take off angle of the photoelectron analyzer was 90° to identify C, N, and O elements.

The surface morphology of scaffolds was examined by Atomic Force Microscopy (AFM) (Dimension 3100 with Nanoscope IIIa controller, Veeco Instruments Inc., CA) in air. AFM images were obtained by scanning surface in a tapping mode (scan size 1×1 μm^2, scan rate 0.95−1.00 Hz) using a silicon nitride probe (model DNP). The spring constant was 0.06 N/m. The root-mean-square (RMS) surface roughness of scaffolds was analyzed using WSXM software.[42]

Cell Culture. Bone marrow hMSCs were purchased from Lonza Bioscience (Singapore) and expanded in mesenchymal stem cell growth medium (MSCGM, Lonza Bioscience). Cells expressed CD 105/+, CD166/+, CD 29/+, CD 44/+, CD 14/−, CD34/−, and CD45/−. Only early passages of hMSCs (passage 4−6) were used for experimental studies. For differentiation experiments, low glucose Dulbecco's Modified Eagle's Medium (DMEM) containing L-glutamine (Sigma Aldrich) supplemented with 10% FBS and 1% antibiotic/antimycotic solution (PAA Laboratories, Australia) was used. Scaffolds in 24-well plate were sterilized by immersing in 70% ethanol for 30 min and then rinsed 2 times with PBS before cell seeding (seeding density was 1000 cells/cm^2). hMSCs were cultured under five distinct cell culture conditions includes (I) PLCL surface and culture medium contained 50 μg/mL full length JAG protein (P+JAG_{50p}); (II) PLCL surface and culture medium contained 50 μg/mL JAG peptide (P+JAG_{50}); (III) PLCL surface immobilized with 5 μg/mL JAG peptide (P-JAG_5); (IV) PLCL surface immobilized with 50 μg/mL JAG peptides (P-JAG_{50}) and (V) PLCL surface alone (PLCL). The cells were maintained at 37 °C in a humidified atmosphere of 5% CO_2. Culture medium was changed every 2−3 days.

Quantitative Real Time Polymerase Chain Reaction (qRT-PCR). The activation of Notch signal and several specific markers associated with myogenic and osteogenic differentiations were assessed by qRT-PCR. After 3 and 10 days of cell culture, the RNA of the cell was isolated with RNeasy mini kit (Qiagen) and synthesized into cDNA (iScript cDNA Synthesis Kits, Bio-Rad). The real-time PCR was performed on a CFX96 real time PCR detection system (Bio-Rad) with KAPA SYBR FAST master mix universal (Kapa Biosystems) as our previous reports.[43,44] Primers specific to the targeted genes were obtained from primer bank and were listed in Table 1. Results presented are fold change expression normalized against the calibrators: GAPDH (glyceraldehyde-3-phosphate dehydrogenase) as the endogenous housekeeping gene.

Immunofluorescence Staining. The expression of myocardial-specific markers was also assessed by immunocytochemistry as our previous reports.[43,45] The primary antibody used was mouse monoclonal anti-cardiac troponin T (cTnT, 1:400, AB33589, Abcam). The secondary antibody used was Alexa Fluor 488 goat anti-mouse IgG (1:500, Molecular probes, Invitrogen). Rat heart tissue slide were used as a positive control. Negative control (in the absence of primary antibody) was performed to validate specific binding of the secondary antibody. F-actin was counterstained with TRITC conjugated phalliodin (1:500, Chemicon). Samples were then observed using a Leica TCS SP5 confocal laser scanning microscope (Leica Microsystems, Wetzlar, Germany).

Table 1. Compiled List of Primers Used in This Study

Genebank accession number	gene target	sequence (5′-3′)
NM 002046	GAPDH	CATGAGAAGTATGACAACAGCCT
		AGTCCTTCCACGATACCAAAGT
NM 017617	Notch-1	GAGGCGTGGCAGACTATGC
		CTTGTACTCCGTCAGCGTGA
NM 005524	Hes-1	AAGAAAGATAGCTCGCGGCAT
		CCAGCACACTTGGGTCTGT
BC 021289	ALPL	CTCTCCAAGACGTACAACACC
		AATGCCCACAGATTTCCCAGC
NM 004348	RUNX2	TCCTATGACCAGTCTTACCCCT
		GGCTCTTCTTACTGAGAGTGGAA
NM 003118	Osteonectin (ON)	AGCACCCCATTGACGGGTA
		GGTCACAGGTCTCGAAAAAGC
NM 002052	GATA-4	CCCAGACGTTCTCAGTCAGTG
		GCTGTTCCAAGAGTCCTGCT
NM 004387	NK2 transcription factor related, locus 5 (Nkx2.5)	CCAAGGACCCTAGAGCCGAA
		ATAGGCGGGGTAGGCGTTAT
NM 000257	β-Myosin Heavy Chain (MHC 7)	CACTGATAACGCTTTTGATGTGC
		TAGGCAGACTTGTCAGCCTCT
NM 000364	Cardiac troponin T (cTnT)	TCTCCGAAACAGGATCAACGA
		GCCCGGTGACTTTAGCCTT

Statistical Analysis. Data are expressed as mean ± SD, unless specified. P values were calculated using one way ANOVA, and a p-value of less than 0.05 was considered to be statistically significant.

RESULTS AND DISCUSSION

Surface Modification of PLCL Scaffolds. PLCL is a common synthetic biodegradable polymer, which has been used for cardiac vascular tissue engineering and not only showed elastic properties comparable to native tissue but also promoted active cellular interaction and degraded in a set time period without toxicity issues.[13] Importantly, some medical devices made from it have been approved by Food and Drug Administration for clinical usage.[46] However, the surface of PLCL scaffolds have to be modified to match the individual functionality demanded. In this report, surface of scaffolds was first activated by plasma treatment, and then AAc was polymerized onto scaffold surface as poly(acrylic acid) (pAAc) to confer carboxylic functional groups on the surface of the scaffold. Subsequently, JAG peptide was immobilized through formation peptide bonds between carboxylic groups on the surface of scaffolds and amine groups in peptides. The series of steps is succinctly illustrated in Figure 1A.

Determination of the Amount of Free Radicals on Scaffold Surfaces. The copolymerization of AAc onto the PLCL surface was initiated via generation of free radicals using oxygen plasma and exposure in air. As shown in Figure1B, the free radical concentration increased with increasing plasma irradiation time, went through a maximum value, and then decreased. The maximum concentration appeared at an irradiation time of 90 s. There are at least two counteracting processes, radical formation and recombination, that could occur during the plasma irradiation. The free radicals generated on the PLCL surface ranged between 2.1 to 5.5 nmol/cm^2, which was more than 6-fold higher than that (0.3 nmol/cm^2) generated in previous report,[47] which may be due to the different gas glow discharges exposed and substrates employed. Nevertheless, the excessive irradiation resulted in the scaffold

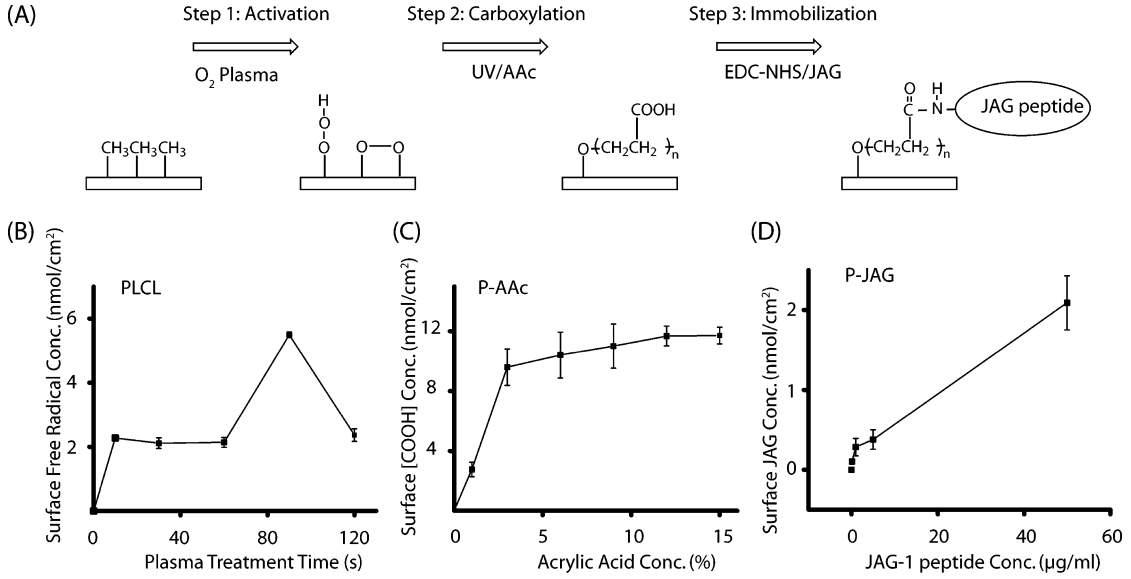

Figure 1. Preparation of JAG peptide immobilized PLCL surface. (A) Illustration of the various steps involved to conjugate JAG peptide onto PLCL scaffold surface. (B) Surface free radical concentration as a function of plasma treatment time. (C) Effect of AAc monomer concentration used for UV polymerization on the surface concentration of the carboxyl groups on the scaffold surface. (D) Effect of JAG peptide concentration used for immobilization on the surface concentration of the peptide on the scaffold surface.

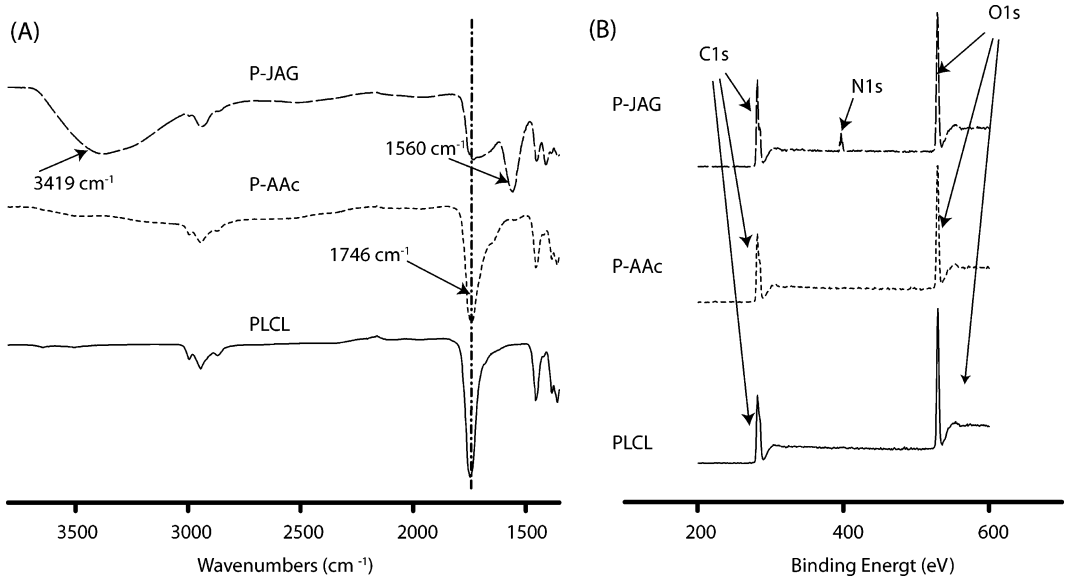

Figure 2. (A) ATR-FTIR spectra of PLCL (continuous line), P-AAc (short dashed line), and P-JAG (long dashed line); (B) XPS wide scanning spectra of PLCL (continuous line), P-AAc (short dashed line), and P-JAG (long dashed line).

being mechanically fragile and melting of the surface, since plasma irradiation can attack the backbone of PLCL and increase scaffold surface temperature. It was measured that the Young's Modulus of scaffold irradiated for 2 min at a power of 100 W decreased by about 11% compared to that of the pristine scaffold (Figure S1, Supporting Information). Therefore, the plasma pretreatment duration for the scaffolds was fixed at 30 s in the following experiments.

Determination of the Carboxyl Group Concentration on Scaffold Surfaces. The yield of AAc grafted on surface of P-AAc was represented by the surface concentration of the carboxyl groups and quantified by TBO assay. Figure 1C showed the influence of monomer concentration used for AAc polymerization on the concentration of the carboxyl groups on the P-AAc surface. The concentration of the carboxyl group increased with the increase of AAc monomer concentration. The most significant increase observed was at monomer concentrations above 3 wt %. Carboxyl group concentration ranging from 2.8 ± 0.5 to 11.7 ± 0.6 nmol/cm^2 could be obtained by varying the initial concentration of the AAc monomer solution from 1% to 15%. The carboxyl group concentration on surface of scaffolds here is lower than those (258 and 560 nmol/cm^2) in previous reports.[38,48] This result was expected as the power of UV light used here (8 W) was much lower than those (1000 and 400 W) in the previous reports.[38,48] 6% AAc monomer solution was chosen to fabricate P-AAc with a carboxyl group density of 10.4 ± 1.5 nmol/cm^2 for the following peptide conjugation.

Determination of the JAG Peptides Concentration on Scaffold Surfaces. JAG peptide immobilized on P-JAG

dx.doi.org/10.1021/am4045635 | ACS Appl. Mater. Interfaces 2014, 6, 1652−1661

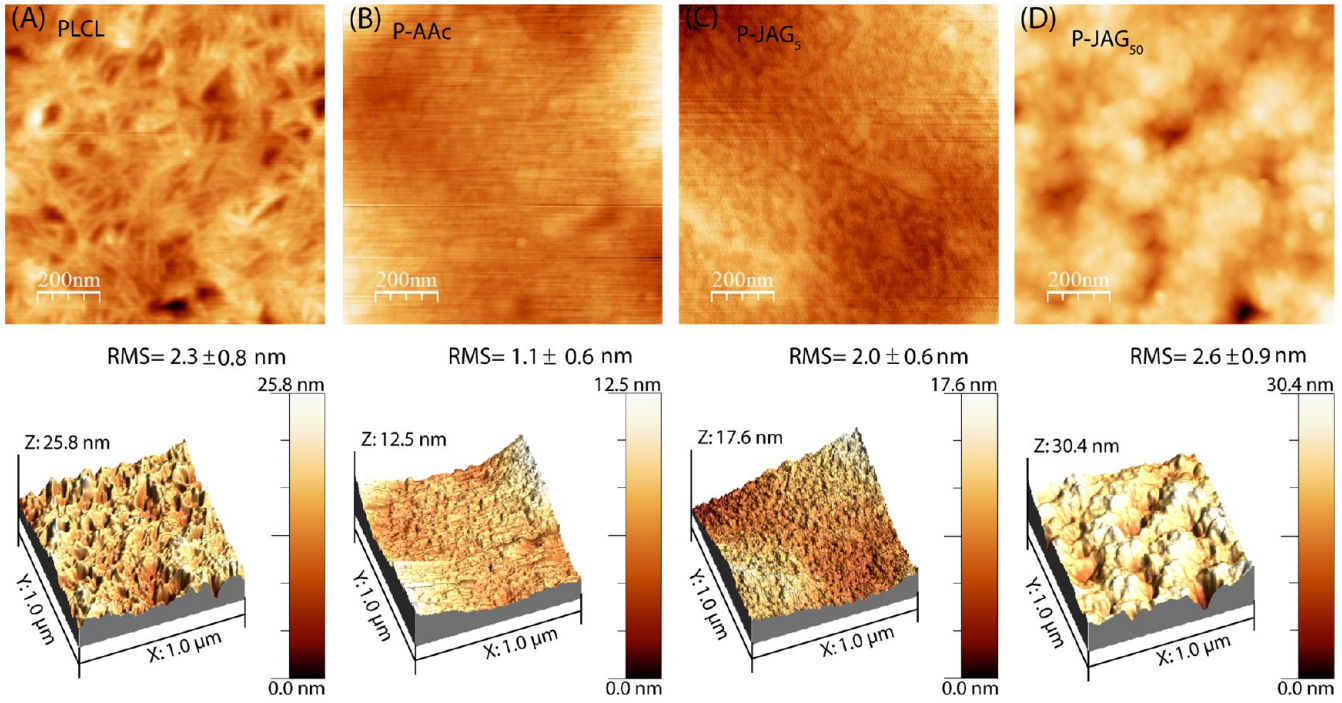

Figure 3. AFM morphological images and root-mean-square roughness (RMS) values of (a) PLCL, (b) P-AAc, (c) P-JAG$_5$, and (d) P-JAG$_{50}$.

surfaces was quantified by XPS. A standard curve (Figure S2, Supporting Information) that defines the relationship between the known concentration of JAG peptide on P-AAc surface and N element concentration was constructed via XPS analysis of known concentration of JAG peptide physically adsorbed on P-AAc surface. Figure 1D showed that the amount of surface JAG peptides immobilized increased with the increasing of JAG peptide concentration used for reaction. The surface JAG peptide concentration from about 102.1 pmol/cm^2 to 2.09 nmol/cm^2 (0.214 to 4.39 μg/cm^2) could be obtained by varying the concentration of the JAG peptides solution from 0.1 to 50 μg/mL (47.62 nM to 23.81 μM). It was reported that scaffold surface immobilization by recombinant full length Jagged-1/Fc protein (0.3 to 18 μg/mL)(1.71 to 102.86 nM) could activate Notch signaling pathway and, therefore, regulated cell fate decisions and cellular differentiation mediated through cell-substrate interactions.[20,34] However, the maximum surface concentrations of JAG protein immobilized were less than 1.1 pmol/cm^2 (0.19 μg/cm^2). Higher concentration of peptide on surface than that of protein was expected as (1) short chain of peptide can decrease the steric hindrance between surface carbonyl groups and primary amine groups in JAG peptides and (2) high concentration of peptide was used in reaction. The PLCL scaffolds immobilized with JAG peptides solution with concentrations of 5 and 50 μg/mL were denoted as P-JAG$_5$ and P-JAG$_{50}$, respectively.

Surface Characterization of Scaffolds. *ATR-FTIR Analysis.* The surface chemistry of various scaffolds was qualitatively characterized by ATR-FTIR. Figure 2A showed the ATR-FTIR spectra of (a) PLCL, (b) P-AAc, and (c) P-JAG, respectively. The intense band at 1746 cm^{-1} corresponding to the carbonyl stretch C═O of carboxyl functional group of PLCL[39] as well as that of side chain of pAAc were found in all spectrum.[49] However, two distinct bands were observed at 1560 and 3419 cm^{-1} in P-JAG spectrum. The band observed at 1560 cm^{-1} is assigned to the N−H bend of primary amines in JAG peptides, and the broad band at 3419 cm^{-1} corresponds to N−H stretch of primary and secondary amines[28] in JAG peptides. Taken together, the ATR-FTIR spectrum suggested that the Jagged-1 peptides were successfully immobilized onto the surface of scaffolds.

XPS Analysis. More information supporting the extent of the surface immobilization was yielded by XPS characterization of the elements on different scaffold surfaces. The XPS wide scan spectrum of the pristine PLCL surface was showed in Figure 2B(a). It revealed that carbon and oxygen signals were present which could be predicted from the chemical structure of PLCL. The spectrum of P-AAc surface in Figure 2B(b) also showed the same peaks as pristine PLCL surface corresponding to C1s and O1s as the same elements in acrylic acid chemical structure. However, a new peak corresponding to N1s appeared on the spectrum of P-JAG surface in Figure 2B(c). This could be due to the amino-group of JAG peptides, which were successfully immobilized on the scaffold surface.

AFM Analysis. The surface topography of the PLCL, P-AAc, P-JAG$_5$, and the P-JAG$_{50}$ was studied by AFM. Figure 3A shows that the surface topography of the scaffolds changes as a result of the acrylic acid polymerization and the subsequent JAG immobilization process.The root-mean-square (RMS) surface roughness of P-AAc (1.1 nm) was lower than pristine PLCL(2.3 nm), implying that the pAAc could exist as an overlayer on the PLCL surface. After immobilization of JAG peptides, the values of surface roughness increased to 2 nm for the P-JAG$_5$ and to 2.6 nm for the P-JAG$_{50}$, which is consistent with previous reports.[28,49] In addition, Figure 3A shows the fibrils texture on the surface of PLCL. After polymerization of acrylic acid onto the surface, the fibrils texture disappeared and this may be due to the fact that the surface is now fully covered with pAAc and their chains formed their own domains, which obscured fibrils on the surface of PLCL scaffold (Figure 3B). Moreover, the images of P-JAG$_5$ and P-JAG$_{50}$ surfaces show that the scaffolds were covered with accumulated round dots

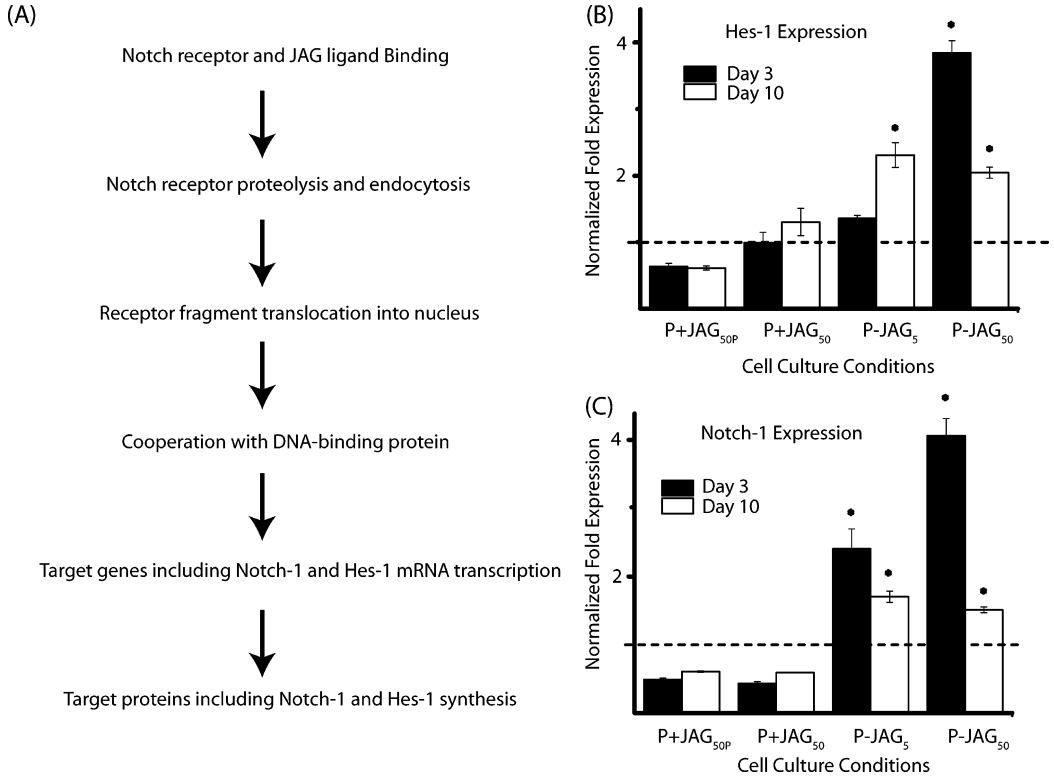

Figure 4. (A) Flow chat of Notch signaling network. (B and C) Relative gene level expression analyses of Hes-1 and Notch-1 markers in hMSCs cultured under five conditions (I) P+JAG$_{50p}$; (II) P+JAG$_{50}$; (III) P-JAG$_5$; (IV) P-JAG$_{50}$; and (V) PLCL on Day 3 and Day 10, respectively. Black and white bars represent samples retrieved on the 3th and 10th day of culture respectively. Bars represent mean ± standard deviation. Relative gene expression levels (i.e., ΔΔCT) were normalized to the control samples indicated by the dashed line. The asterisks indicates statistical significance ($p < 0.05$) difference with control group (PLCL, negative JAG control).

texture, which could result from the peptides conjugated (Figure 3C and D).

Biological Activities of hMSCs Cultured on Scaffolds Surfaces. *Activation of Notch Signaling in hMSCs on P-JAG Surface.* The Notch pathway is a highly conserved signaling mechanism involved in many processes determining cell fate during mammalian cardiac development through local cell interactions. After activation, the Notch intracellular domain is translocated into the nucleus and activates target genes such as Notch-1 and Hes-1 as shown in the flowchart in Figure 4. To examine the efficacy of the immobilized form of JAG peptide in the activation of the Notch signaling cascade in hMSCs, qRT-PCR was used to assess expression level of gene targets that are intimately linked to the activation of Notch signaling cascade such as Hes-1 and Notch-1 in hMSCs cultured under (I) P+JAG$_{50p}$; (II) P+JAG$_{50}$; (III) P-JAG$_5$; (IV) P-JAG$_{50}$; and (V) PLCL. Figure 4B and C showed that the fold of gene expressions of Hes-1 and Notch-1 in cells cultured under P-JAG$_5$ and P-JAG$_{50}$ conditions were up-regulated to 1.4 and 3.9 on Day 3 and 2.3 and 2.1 on Day 10, while down-regulated or maintained as usual under P+JAG$_{50p}$ and P+JAG$_{50}$ conditions. Our results suggested that the Notch signaling in cells can only be activated under the condition that JAG peptide was in its immobilized form and the response is dose dependent. Such activation of the Notch signaling pathway may be explained as follows: (1) only highly concentrated localized ligands at the interface between cells and scaffolds resulted from ligands surface immobilization will overcome the threshold to induce proteolysis and activate the signaling pathway;[37,50] (2) multivalent of immobilized ligands as a result of high localized concentration of ligands are able to enhance the formation of ligand−receptor complex and prevent lateral diffusion of complex;[37] (3) interaction between endogenous and exogenous ligands. At low doses, the soluble ligand sequester the other ligands in homotypic form to effectively reduce the amount of free ligands and serve as an antagonist effect. At high doses, endogenous ligands have been saturated and produce a pure agonist effect as all exogenous ligands are free to react with Notch.[25]

Modulated Myogenic Differentiation of hMSCs on P-JAG Surface. To examine the effect of surface immobilization on lineage commitment of hMSCs, several specific markers associated with myogenic and osteogenic differentiation were selected to assess by qRT-PCR and Immunocytochemistry. GATA-4, Nkx2.5, MYH7, and cTnT were used as the markers to indicate myogenic differentiations. GATA-4 is a zinc-finger transcription factor that acts as a critical early regulator of the cardiac differentiation. In addition, GATA-4 has been also identified in stem and progenitor cells of the heart in combination with stemness markers. NK2 transcription factor related, locus 5 (Nkx2.5) functions in heart formation and development. Same as GATA-4, Nkx2.5 was viewed as the early determinant of myocyte formation.[51] In Figure 5A and B, it was found that the fold of gene expressions of GATA-4 were.1.5, 3.8 on Day 3 and both increased to 5.5, 8.2 on Day 10 when cells were cultured under P-JAG$_5$ and P-JAG$_{50}$ conditions, respectively. Similarly, the fold change expression level of Nkx2.5 were 1.4, 4.9 on Day 3 and 3.2, 4.5 on Day 10 for cells cultured under P-JAG$_5$ and P-JAG$_{50}$ conditions. In stark contrast, the expressions of myogenic genes in cells cultured

dx.doi.org/10.1021/am4045635 | ACS Appl. Mater. Interfaces 2014, 6, 1652−1661

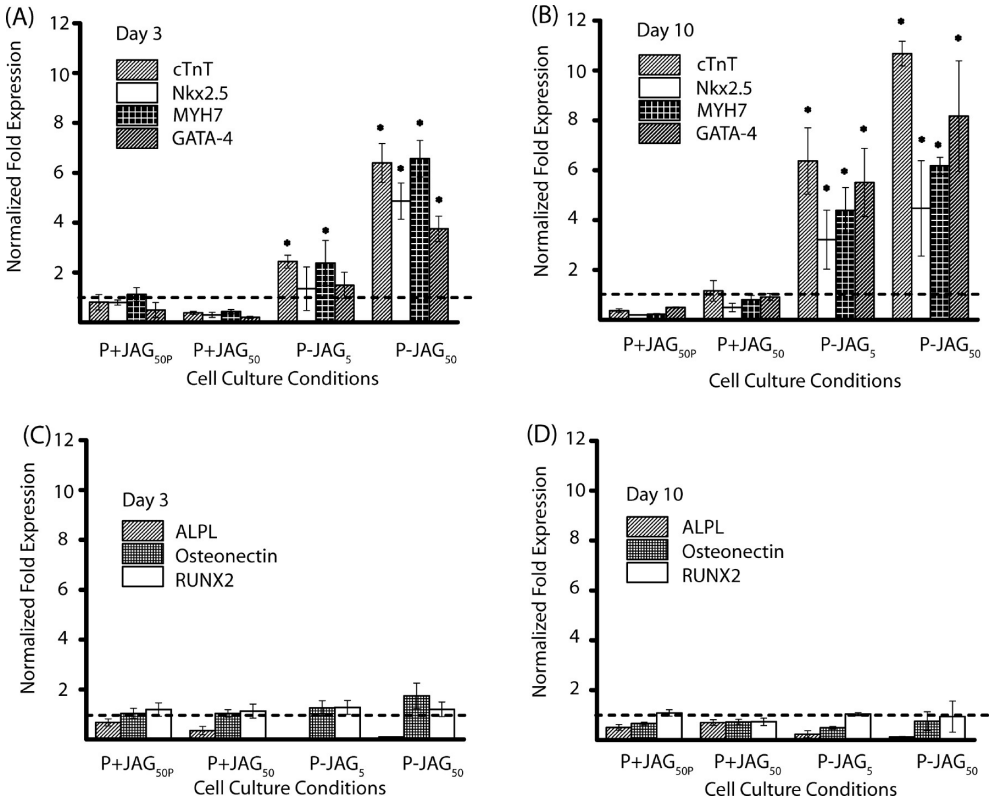

Figure 5. Relative gene level expression analyses of (A, B) myogenic and (C, D) osteogenic markers in hMSCs cultured under five conditions (I) P+JAG_{50p}; (II) P+JAG_{50}; (III) P-JAG_5; (IV) P-JAG_{50}; and (V) PLCL on Day 3 and Day 10, respectively. Bars represent mean ± standard deviation. Relative gene expression levels (i.e. ΔΔCT) were normalized to the control samples indicated by the dashed line. The asterisks indicates statistical significance ($p < 0.05$) difference with control groups (PLCL, negative JAG control).

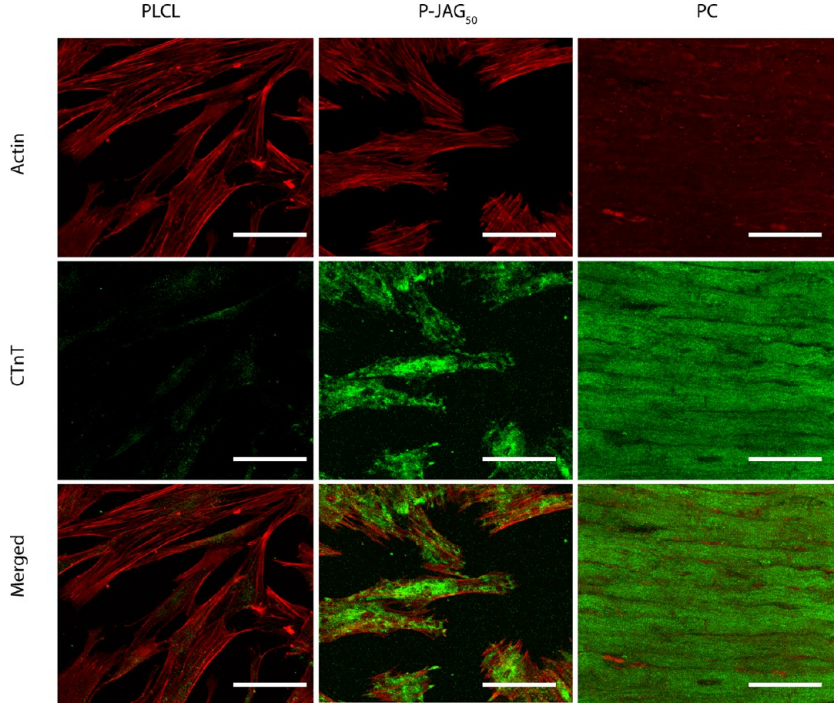

Figure 6. Representative images showing immunostaining of the myogenic marker on hMSCs cultured under PLCL; P-JAG_{50}; and positive control (PC) (rat heart tissue slide). Cells were stained with a distinctive and mature marker of myogenic differentiations using mouse monoclonal anti-cardiac troponin T(cTnT)(green). F-actin was counterstained with TRITC conjugated phalliodin (red). Scale bar =100 μm.

under condition P+JAG_{50p} and P+JAG_{50} remained at nominal levels. The MYH7 gene encodes a protein known as the cardiac β-myosin heavy chain, and cTnT is one of protein subunits in Troponin complex located on the thin filament of the

dx.doi.org/10.1021/am4045635 | ACS Appl. Mater. Interfaces 2014, 6, 1652−1661

myocardial contractile apparatus. All of them play critical roles in the cardiac muscle functionality of the contractile machinery cooperatively.[52] They were viewed as the late stage marker of myocyte differentiation. In Figure 5A and B, it was found that the fold of expression of MYH7 were 2.4, 6.6 on Day 3 and 4.4, 6.2 on Day 10 when cells were cultured in two peptide immobilized scaffolds, respectively. Same as MYH7, the folds of expression of Nkx2.5 were 1.4, 4.9 on Day 3 and both increased to 6.4, 10.7 on Day 10 when cells were cultured in two peptide immobilized scaffolds, respectively. On the contrary, the expression level of MYH7 and Nkx2.5 of cells cultured under condition P+JAG_{50p} and P+JAG_{50} remained at nominal levels. Overall, mRNAs levels of these markers associated with myogenic differentiation were up-regulated for cells cultured in peptide immobilized scaffolds.

ALPL, RUNX2, and Osteonectin were selected as the markers indicative of osteogenic differentiation. Alkaline phosphatase, an ectoenzyme encoded by the ALPL gene, is believed to be critical for bone matrix mineralization and is the most widely recognized marker of osteoblast phenotypes.[53] RUNX2, a basic helix loop helix transcription factor is also indicative of osteogenic differentiation from the onset of bone mineralization.[43] The upregulation of osteonectin gene expression was used as an early marker to indicated hMSCs toward osteogenic differentiation in previous report.[54] The difference in fold change in the expressions of selected osteo-specific genes during the osteogenic differentiation were recorded on Day 3 and Day 10 as shown in Figure 5 C-D. The fold change expressions of these three markers were not significantly different compared to the control on Day 3 and Day 10. In general, osteogenic genes did not show any significant up-regulation compared to the control during 10-day cell culture under all cell culture conditions. Taken together, mRNAs levels of these markers associated with myogenic differentiation were up-regulated for cells cultured in peptide immobilized scaffolds, while they remained as nominal levels in controls. On the contrary, mRNAs levels of markers associated with osteogenic differentiation remained unchanged. Collectively, our findings suggest that JAG peptides modified surface seems to be capable of directing stem cell lineage commitment of hMSCs, particularly toward the myogenic lineage.

To further investigate whether the up-regulation of mRNA expression of specific gene associated with myogenic differentiation is sufficient to trigger hMSCs commitment toward the particular cell lineage at the protein level, we performed immunofluorescent staining to confirm the phenotypes of hMSCs cultured in peptide immobilized scaffolds in concordance with gene expression result. As shown in Figure 6, positive cTnT staining was detected from cells in peptides immobilized scaffolds after 10 days of cell culture. However, cTnT staining only showed a diffused cytoplasmic distribution and lack of cross-striating Z-bands indicating a partially differentiated phenotype.[55] Collectively, these results indicated that the JAG peptide immobilized scaffolds would activate Notch signaling pathway and modulate hMSCs myogenic differentiation but without initiating osteogenic differentiation.

The importance of the Notch pathway on cells proliferation and differentiation has been extensively investigated; however, the evidence were contradictory. For example, it was reported that activated Notch inhibits myogenic activity through specifically blocking DNA binding by MEF2C in embryonic mesenchymal cell line 10T1/2.[56] However, it was also reported that Notch signaling facilitates the in vitro differentiation of BM-derived cells into SM-like cells during arterial lesion formation.[57] In certain scenarios, Notch maintains an undifferentiated state of progenitors,[22] whereas in others Notch produces inductive signaling that stimulates progenitors to specific fate.[20] The possible reason is that the Notch signaling is exquisitely sensitive to dosage, developmental timing, and cellular context. Our result could be explained according to previous finding that activation of Notch signaling could promote myogenic differentiation of cells possibly through target gene Nkx2.5,[23] while suppressing osteogenic differentiation.[22] In the cardiac tissue regenerative medicine field, considerable interest has been devoted toward the design of novel cardiac patches with the aim to efficiently deliver cell into infarcted area to inhibit heart remodelling and promote cardiomyocytes proliferation. Herein, we report for the first time the use of JAG peptide immobilized on biodegradable polymeric cardiac patch, which serves as a powerful artificial stem cell niche to direct stem cell fate. In addition, besides the effect on myogenic differentiation induction, it was previously reported that injection of MSC overexpressing Notch intracellular domain leads to decreased infarct size and improved cardiac function.[58] The effect of this functionalized cardiac patch in in vivo study and the details of signaling pathway for the observed phenomenon would be of interest for future studies.

CONCLUSIONS

We engineered the surface of a biodegradable polymeric scaffold through immobilization of JAG peptides. Consequently, Notch signaling was triggered in hMSCs cultured on the engineered surface. Evidence from gene expression analysis showed that immobilization of JAG peptide is essential for activation of Notch signaling pathway in hMSCs. Furthermore, gene expression and immunocytochemistry analysis revealed that the scaffolds immobilized with JAG peptides favor the differentiation of hMSCs into myocyte-like cells. Therefore, this strategy is not only useful to dissect the molecular events leading up to pro-myogenic effects of hMSCs, but enhances the functional potential of scaffolds to be used as a bioengineered cardiac patch in myocardial infarction repair.

ASSOCIATED CONTENT

Supporting Information

Effect of plasma treatment on PLCL mechanical property, standard curve for XPS experiment, gene expression of myogenic markers in hMSCs cultured on P-AAc and immunostaining of the myogenic marker of hMSCs cultured under P+JAG_{50p}; P+JAG_{50} and P-JAG_5. These materials are available free of charge via the Internet at http://pubs.acs.org.

AUTHOR INFORMATION

Corresponding Author

* Tel.: +65 67906186. Fax: +65 67909081. E-mail: lptan@ntu.edu.sg.

Present Address

[§]Department of Chemical and Biomolecular Engineering, National University of Singapore, Singapore.

Notes

The authors declare no competing financial interest.

■ ACKNOWLEDGMENTS

The authors thank National Research Foundation (Grant No: NRF-CRP2-2007-1) and Singapore Stem Cell Consortium (SSCC) (Grant No: SSCC/09/017) for their financial support.

■ REFERENCES

(1) Laflamme, M. A.; Murry, C. E. *Nature* **2011**, *473*, 326−335.
(2) Radisic, M.; Park, H.; Vunjak-Novakovic, G. Cardiac-Tissue Engineering. In *Principles of Tissue Engineering*, 3rd ed.; Robert, L.; Robert, L.; Joseph, V., Eds.; Academic Press: Burlington, 2007; pp 551−567.
(3) Segers, V. F. M.; Lee, R. T. *Nature* **2008**, *451*, 937−942.
(4) Large, S. *Heart* **2007**, *93*, 392−402.
(5) Perin, E. C.; Silva, G. H.; Willerson, J. Stem Cell Therapy for Cardiac Diseases. In *Cardiovascular Medicine*, 3rd ed.; Willerson, J.; Wellens, H. J.; Cohn, J.; Holmes, D., Jr., Eds.; Churchill Livingstone: Philadelphia, 2007; pp 2745−2769.
(6) Orlic, D.; Kajstura, J.; Chimenti, S.; Jakoniuk, I.; Anderson, S. M.; Li, B.; Pickel, J.; McKay, R.; Nadal-Ginard, B.; Bodine, D. M.; Leri, A.; Anversa, P. *Nature* **2001**, *410*, 701−705.
(7) Ankrum, J.; Karp, J. M. *Trends Mol. Med.* **2010**, *16*, 203−209.
(8) Chen, F. H.; Song, L.; Mauck, R. L.; Li, W.-J.; Tuan, R. S. Mesenchymal Stem Cells. In *Principles of tissue engineering*, 3rd ed.; Lanza, R.; Langer, R.; Vacanti, J., Eds. Academic Press: Burlington, MA, 2007; pp 823−843.
(9) Schächinger, V.; Erbs, S.; Elsässer, A.; Haberbosch, W.; Hambrecht, R.; Hölschermann, H.; Yu, J.; Corti, R.; Mathey, D. G.; Hamm, C. W.; Süselbeck, T.; Assmus, B.; Tonn, T.; Dimmeler, S.; Zeiher, A. M. *N. Engl. J. Med.* **2006**, *355*, 1210−1221.
(10) Bartunek, J.; Sherman, W.; Vanderheyden, M.; Fernandez-Aviles, F.; Wijns, W.; Terzic, A. *Clin. Pharmacol. Ther.* **2009**, *85*, 548−552.
(11) Madden, L. R.; Mortisen, D. J.; Sussman, E. M.; Dupras, S. K.; Fugate, J. A.; Cuy, J. L.; Hauch, K. D.; Laflamme, M. A.; Murry, C. E.; Ratner, B. D. *Proc. Natl. Acad. Sci. U.S.A.* **2010**, *107*, 15211−15216.
(12) Miyahara, Y.; Nagaya, N.; Kataoka, M.; Yanagawa, B.; Tanaka, K.; Hao, H.; Ishino, K.; Ishida, H.; Shimizu, T.; Kangawa, K.; Sano, S.; Okano, T.; Kitamura, S.; Mori, H. *Nat. Med.* **2006**, *12*, 459−465.
(13) Jin, J.; Jeong, S. I.; Shin, Y. M.; Lim, K. S.; Shin, H. s.; Lee, Y. M.; Koh, H. C.; Kim, K. S. *Eur. J. Heart Fail.* **2009**, *11*, 147−153.
(14) Quevedo, H. C.; Hatzistergos, K. E.; Oskouei, B. N.; Feigenbaum, G. S.; Rodriguez, J. E.; Valdes, D.; Pattany, P. M.; Zambrano, J. P.; Hu, Q.; McNiece, I.; Heldman, A. W.; Hare, J. M. *Proc. Natl. Acad. Sci. U.S.A.* **2009**, *106*, 14022−14027.
(15) Breitbach, M.; Bostani, T.; Roell, W.; Xia, Y.; Dewald, O.; Nygren, J. M.; Fries, J. W. U.; Tiemann, K.; Bohlen, H.; Hescheler, J.; Welz, A.; Bloch, W.; Jacobsen, S. E. W.; Fleischmann, B. K. *Blood* **2007**, *110*, 1362−1369.
(16) Godier-Furnémont, A. F. G.; Martens, T. P.; Koeckert, M. S.; Wan, L.; Parks, J.; Arai, K.; Zhang, G.; Hudson, B.; Homma, S.; Vunjak-Novakovic, G. *Proc. Natl. Acad. Sci. U.S.A.* **2011**, *108*, 7974−7979.
(17) Tay, C. Y.; Irvine, S. A.; Boey, F. Y. C.; Tan, L. P.; Venkatraman, S. *Small* **2011**, *7*, 1361−1378.
(18) Niessen, K.; Karsan, A. *Circ. Res.* **2008**, *102*, 1169−1181.
(19) Nemir, M.; Pedrazzini, T. *J. Mol. Cell Cardiol.* **2008**, *45*, 495−504.
(20) Beckstead, B. L.; Tung, J. C.; Liang, K. J.; Tavakkol, Z.; Usui, M. L.; Olerud, J. E.; Giachelli, C. M. *J. Biomed. Mater. Res., Part A* **2009**, *91A*, 436−446.
(21) Bray, S. J. *Nat. Rev. Mol. Cell Biol.* **2006**, *7*, 678−689.
(22) Hilton, M. J.; Tu, X.; Wu, X.; Bai, S.; Zhao, H.; Kobayashi, T.; Kronenberg, H. M.; Teitelbaum, S. L.; Ross, F. P.; Kopan, R.; Long, F. *Nat. Med.* **2008**, *14*, 306−314.
(23) Boni, A.; Urbanek, K.; Nascimbene, A.; Hosoda, T.; Zheng, H.; Delucchi, F.; Amano, K.; Gonzalez, A.; Vitale, S.; Ojaimi, C.; Rizzi, R.; Bolli, R.; Yutzey, K. E.; Rota, M.; Kajstura, J.; Anversa, P.; Leri, A. *Proc. Natl. Acad. Sci. U. S. A.* **2008**, *105*, 15529−15534.
(24) Li, H.; Yu, B.; Zhang, Y.; Pan, Z.; Xu, W.; Li, H. *Biochem. Biophys. Res .Commun.* **2006**, *341*, 320−325.
(25) Zlobin, A.; Jang, M.; Miele, L. *Curr. Pharm. Biotechnol.* **2000**, *1*, 83−106.
(26) Lutolf, M. P.; Gilbert, P. M.; Blau, H. M. *Nature* **2009**, *462*, 433−441.
(27) Alberti, K.; Davey, R. E.; Onishi, K.; George, S.; Salchert, K.; Seib, F. P.; Bornhauser, M.; Pompe, T.; Nagy, A.; Werner, C.; Zandstra, P. W. *Nat. Methods* **2008**, *5*, 645−650.
(28) Yue, Z.; Liu, X.; Molino, P. J.; Wallace, G. G. *Biomaterials* **2011**, *32*, 4714−4724.
(29) Engler, A. J.; Sen, S.; Sweeney, H. L.; Discher, D. E. *Cell* **2006**, *126*, 677−689.
(30) Miyagi, Y.; Chiu, L. L. Y.; Cimini, M.; Weisel, R. D.; Radisic, M.; Li, R. K. *Biomaterials* **2011**, *32*, 1280−1290.
(31) Kim, M. H.; Kino-oka, M.; Maruyama, N.; Saito, A.; Sawa, Y.; Taya, M. *Biomaterials* **2010**, *31*, 7666−7677.
(32) Zweidler-McKay, P. A.; He, Y.; Xu, L.; Rodriguez, C. G.; Karnell, F. G.; Carpenter, A. C.; Aster, J. C.; Allman, D.; Pear, W. S. *Blood* **2005**, *106*, 3898−3906.
(33) Nickoloff, B.; Qin, J. Z.; Chaturvedi, V.; Denning, M.; Bonish, B.; Miele, L. *Cell Death Differ.* **2002**, *9*, 842−855.
(34) Gonçalves, R. M.; Martins, M. C. L.; Almeida-Porada, G.; Barbosa, M. A. *Biomaterials* **2009**, *30*, 6879−6887.
(35) Toda, H.; Yamamoto, M.; Kohara, H.; Tabata, Y. *Biomaterials* **2011**, *32*, 6920−6928.
(36) Beckstead, B. L.; Santosa, D. M.; Giachelli, C. M. *J. Biomed. Mater. Res., Part A* **2006**, *79A*, 94−103.
(37) Ito, Y. *Soft Matter* **2008**, *4*, 46−56.
(38) Ying, L.; Yin, C.; Zhuo, R. X.; Leong, K. W.; Mao, H. Q.; Kang, E. T.; Neoh, K. G. *Biomacromolecules* **2002**, *4*, 157−165.
(39) Li, H.; Wen, F.; Wong, Y. S.; Boey, F. Y. C.; Subbu, V. S.; Leong, D. T.; Ng, K. W.; Ng, G. K. L.; Tan, L. P. *Acta Biomater.* **2012**, *8*, 531−539.
(40) Du, Y.; Han, R.; Wen, F.; Ng San San, S.; Xia, L.; Wohland, T.; Leo, H. L.; Yu, H. *Biomaterials* **2008**, *29*, 290−301.
(41) Wang, Y.; Kim, J. H.; Choo, K. H.; Lee, Y. S.; Lee, C. H. *J. Membr. Sci.* **2000**, *169*, 269−276.
(42) Horcas, I.; Fernández, R.; Gómez-Rodríguez, J. M.; Colchero, J.; Gómez-Herrero, J.; Baro, A. M. *Rev. Sci. Instrum.* **2007**, *78*, 013705−1−8.
(43) Tay, C. Y.; Yu, H.; Pal, M.; Leong, W. S.; Tan, N. S.; Ng, K. W.; Leong, D. T.; Tan, L. P. *Exp. Cell. Res.* **2010**, *316*, 1159−1168.
(44) Tay, C. Y.; Pal, M.; Yu, H.; Leong, W. S.; Tan, N. S.; Ng, K. W.; Venkatraman, S.; Boey, F.; Leong, D. T.; Tan, L. P. *Small* **2011**, *7*, 1416−1421.
(45) Yu, H.; Lui, Y. S.; Xiong, S.; Leong, W. S.; Wen, F.; Nurkahfianto, H.; Rana, S.; Leong, D. T.; Ng, K. W.; Tan, L. P. *Stem Cells Dev.* **2013**, *22*, 136−147.
(46) Klopp, L. S.; Simon, B. J.; Bush, J. M.; Enns, R. M.; Turner, A. S. *Spine* **2008**, *33*, 1518−1526.
(47) Suzuki, M.; Kishida, A.; Iwata, H.; Ikada, Y. *Macromolecules* **1986**, *19*, 1804−1808.
(48) Du, Y.; Chia, S. M.; Han, R.; Chang, S.; Tang, H.; Yu, H. *Biomaterials* **2006**, *27*, 5669−5680.
(49) Cheng, Z.; Teoh, S. H. *Biomaterials* **2004**, *25*, 1991−2001.
(50) Varnum-Finney, B.; Wu, L.; Yu, M.; Brashem-Stein, C.; Staats, S.; Flowers, D.; Griffin, J. D.; Bernstein, I. D. *J. Cell Sci.* **2000**, *113*, 4313−4318.
(51) Olson, E. N. *Science* **2006**, *313*, 1922−1927.
(52) Junqueira, L. C.; Carneiro, J. *Basic Histology: Text & Atlas*, 10th ed.; Lange Medical Books McGraw-Hill: Singapore, 2003; pp 191−215.
(53) Wen, F.; Magalhães, R.; Gouk, S. S.; Gajadhar, B.; Lee, K. H.; Hutmacher, D. W.; Kuleshova, L. L. *Tissue Eng., Part C* **2009**, *15*, 105−114.
(54) Zhao, F.; Grayson, W. L.; Ma, T.; Irsigler, A. *J. Cell. Physiol.* **2009**, *219*, 421−429.

(55) Tan, G.; Shim, W.; Gu, Y.; Qian, L.; Ying Chung, Y.; Yun Lim, S.; Yong, P.; Sim, E.; Wong, P. *Differentiation* **2010**, *79*, 260−271.
(56) Wilson-Rawls, J.; Molkentin, J. D.; Black, B. L.; Olson, E. N. *Mol. Cell. Biol.* **1999**, *19*, 2853−2862.
(57) Doi, H.; Iso, T.; Shiba, Y.; Sato, H.; Yamazaki, M.; Oyama, Y.; Akiyama, H.; Tanaka, T.; Tomita, T.; Arai, M.; Takahashi, M.; Ikeda, U.; Kurabayashi, M. *Biochem. Biophys. Res. Commun.* **2009**, *381*, 654−659.
(58) Li, Y.; Hiroi, Y.; Ngoy, S.; Okamoto, R.; Noma, K.; Wang, C. Y.; Wang, H. W.; Zhou, Q.; Radtke, F.; Liao, R.; Liao, J. K. *Circulation* **2011**, *123*, 866−876.